Acta Cryst. (1999). B**55**, 788–792

On the polymorphism of a sapogenin monohydrate induced by different rotations of water molecules

László Fábián, Gyula Argay and Alajos Kálmán*

Institute of Chemistry, Chemical Research Center, Hungarian Academy of Sciences, Budapest 114, PO Box 17, H-1525, Hungary. E-mail: akalman@cric.chemres.hu

(*Received 16 September 1998; accepted 14 April 1999*)

Abstract

The structure of 1β,3β,11α-trihydroxyspirosta-5,25(27)-diene ($C_{27}H_{40}O_5$; a steroidal sapogenin) isolated from *Helleborus serbicus* Adam 1906 (Ranunculaceae) and crystallized from absolute ethanol as a monohydrate (melting point 519–522 K) had been characterized by two symmetry-independent binary (steroid–water) layers, cross-linked by hydrogen bonds [Kálmán *et al.* (1985). *Acta Cryst.* C**41**, 1645–1647]. Recently, a novel monohydrate was crystallized again from absolute ethanol (source: *Helleborus multifidus* subspecies *serbicus*) with a somewhat higher melting point of 525–526 K. X-ray analysis of these crystals [Argay *et al.* (1998). *Acta Chim. Hung.* **135**, 449–456] revealed a novel polymorph (hereinafter denoted polymorph ***B***), which is also built up by two binary layers of $C_{27}H_{40}O_5$ and H_2O, but in which the relative position of these layers differs from that found in the first modification (polymorph ***A***). Comparing the two polymorphs, layers of one type are found to be similar, displaying identical hydrogen bonding, whereas layers of the second type differ with respect to the orientations adopted by the water molecules; these orientations also differ from those in the layers of the first type. Consequently, by these water rotations, hydrogen bonds, at least partly, are reversed. This leads to two different close packings: in form ***A*** four consecutive layers are cross-linked by two homomolecular (hydroxyl···hydroxyl and water···water) hydrogen-bond pairs, while in ***B*** there are only heteromolecular hydroxyl···water bonds. These hydrogen-bond dissimilarities together with the differences in the weak CH···*X etc*. interactions explain the greater stability of the higher melting-point form ***B***.

1. Introduction

For many years a Serbian team (Vladimirov *et al.*, 1991) has been seeking practically applicable sources of steroidal sapogenins by testing different *Helleborus* species (*e.g. atrorubens*, *odorus*, *niger* and *serbicus*). First, as a main component, 1β,3β,11α-trihydroxyspirosta-5,25(27)-diene was isolated from *Helleborus serbicus* Adam 1906 and crystallized from absolute ethanol as a monohydrate. Crystals with a melting point of 519–522 K were subjected to X-ray diffractometry (Philips PW1100 diffractometer) in Zagreb by Ribár (1984), while the structure was solved in Budapest and reported by Kálmán *et al.* (1985). Subsequently, a related sapogenin, 3β,11α-dihydroxyspirosta-5,25(27)-diene, was

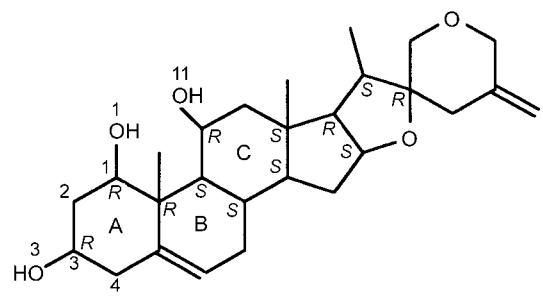

also isolated and purified. It crystallized in anhydrous form with a melting point of 496–498K (Ribár *et al.*, 1986). Years later the ongoing study of *Helleborus* plants yielded a new source (*H. multifidus* subspecies *serbicus*) of these sapogenins (Vladimirov *et al.*, 1991). 1β,3β,11α-Trihydroxyspirosta-5,25(27)-diene, after extraction and purification by layer chromatography, again crystallized from absolute ethanol as a monohydrate, but with a melting point of 525–526K. X-ray study of these crystals (data collected on a CAD-4 diffractometer) performed in Budapest revealed a novel form (Argay *et al.*, 1998) of the sapogenin monohydrate. Crystal data of both polymorphs, each with two molecular associates of $C_{27}H_{40}O_5.H_2O$ in the asymmetric unit, are as follows.

(*a*) Form ***A*** melts at 519–521 K. Crystals are monoclinic, space group $P2_1$, with a = 10.085 (4), b = 7.854 (2), c = 31.956 (15) Å, β = 93.11 (3)°, V = 2527.4 (17) Å^3, Z = 4 (R_1 = 0.038 for 4262 reflections). Since no more crystals of the sample sent to Zagreb for X-ray diffraction analysis are available, a refinement of the original data set was repeated in F^2 mode. The result (Argay *et al.*, 1998) was in agreement with the structure reported earlier (Kálmán *et al.*, 1985); thus the present work refers to the original atomic coordinates.

(*b*) Form ***B*** melts at 525–526 K. Crystals are also monoclinic, space group $P2_1$, with a = 13.033 (1), b =

8.314 (1), c = 23.823 (2) Å, β = 105.17 (1)°, V = 2491.4 (4) Å^3, Z = 4 (R_1 = 0.036, wR_2 = 0.104 for 10 287 reflections).

In accordance with our knowledge on polymorphism (Haleblian, 1975; Threlfall, 1995), the smaller unit-cell volume (by 1.4%) and the higher melting point suggest that form ***B*** is somewhat more stable than form ***A***. Since the Serbian team (Vladimirov, 1998) did not preserve crystals from the first sample (***A***) studied by X-rays in Zagreb, no further investigations [*e.g.* as to whether the transition between forms ***A*** and ***B*** is enantiotropic or monotropic (Threlfall, 1995)] could be performed without new plant collections. Monotropic phase transition would mean a disappearing polymorph (Dunitz & Bernstein, 1995). To check disappearing and reappearing polymorphism (Bernstein & Henck, 1998), *e.g.* like that of the low-melting-point (monoclinic) form of 1,2,3,5-tetra-*O*-acetyl-β-D-ribofuranose described in detail by Czugler *et al.* (1981), a few microgrammes of ***B*** (all that is available) is insufficient. It does not permit such controlled crystallizations as that of famotidine, of which industrial amounts enabled Hegedüs *et al.* (1989) to reproduce both the kinetically and the thermodynamically preferred polymorphs. Similarly, fast and slow cooling of acetazolamide, using 20 g of material, yielded two modifications, I and II, from water (Griesser *et al.*, 1997). At any rate, in accordance with the remarkable structural similarities observed and with the close melting points of dimorphs ***A*** and ***B***, depending on minor differences in the crystallization, the formation of any of them may occur. This possibility cannot be disproved at present. Of course, contamination effects, *e.g.* the presence of a small amount of 3β,11α-dihydroxyspirosta-5,25(27)-diene (Ribár *et al.*, 1986; Vladimirov *et al.*, 1991), cannot be excluded either.

2. Discussion

2.1. *Layer structure*

In both dimorphs ***A*** and ***B*** the symmetry-independent binary layers (*A*1/*A*2 and *B*1/*B*2) are held together by infinite [O(W)—H···O3^a—H3^a···O(W^b)—H^b] chains of hydrogen-bonded rings formed around the twofold screw axes (Fig. 1) separated by *a*/2. The hydrophilic region of the steroid molecules, represented by ring A

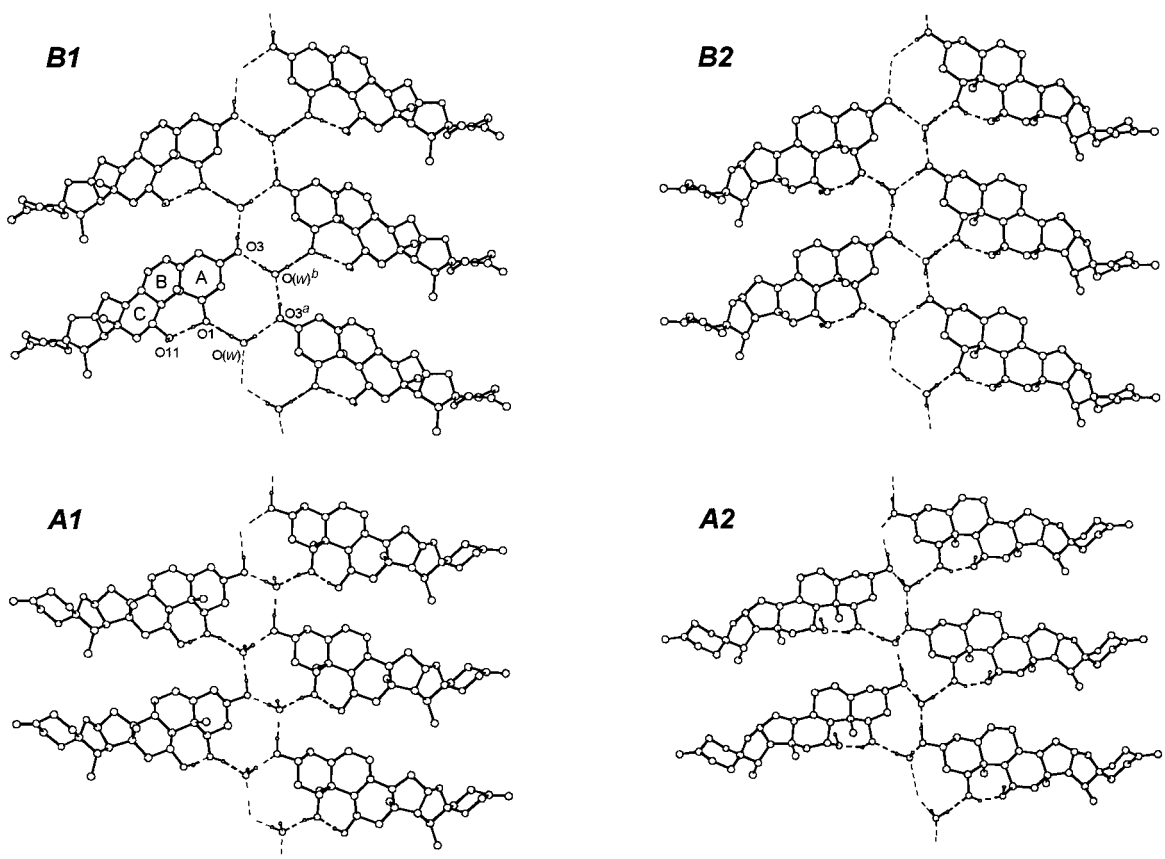

Fig. 1. Symmetry-independent layers in the polymorphs: *A*1, *A*2, *B*1 and *B*2. Each layer is fused together by an infinite $C_2^2(4)$ chain of [O(W)—H···O3^a—H^a···O(W^b)—H^b] hydrogen bonding along the screw axis lying in the plane of the paper. Superscripts *a* ($y-\frac{1}{2}$) and *b* ($y+\frac{1}{2}$) refer to the directions in the translation of 2_1. Only relevant atoms and rings are labelled.

Table 1. *Hydrogen bonds in polymorphs **A** and **B***

Primes in atom labels denote atoms of layers *A*2 and *B*2, respectively.

D—H···*A*	H···*A* (Å)	*D*···*A* (Å)	*D*—H···*A* (°)
Polymorph ***A***			
O1—H1···O(*W*)	1.84 (3)	2.796 (5)	170 (2)
O1—H1···O(*W*)	1.84 (3)	2.796 (5)	170 (2)
O3—H3···O(*W*)^{i}	2.02 (5)	2.816 (5)	175 (4)
O11—H11···O1	1.61 (3)	2.602 (5)	171 (2)
O(*W*)—H*a*···O(*W′*)^{ii}	1.95 (4)	2.804 (5)	175 (3)
O(*W*)—H*b*···O3^{iii}	2.12 (2)	2.785 (5)	170 (4)
O1′—H1′···O11′	1.87 (3)	2.600 (5)	149 (3)
O3′—H3′···O(*W′*)^{i}	2.15 (5)	2.792 (5)	139 (4)
O11′—H11′···O11	1.99 (4)	2.879 (5)	174 (3)
O(*W′*)—H*a′*···O1′	1.93 (4)	2.803 (5)	153 (2)
O(*W′*)—H*b′*···O3′^{iv}	2.08 (4)	2.780 (5)	170 (4)
Polymorph ***B***			
O1—H1···O11	1.68 (2)	2.556 (2)	172 (3)
O3—H3···O(*W*)^{v}	1.93 (2)	2.785 (2)	169 (3)
O11—H11···O(*W′*)^{vi}	1.90 (2)	2.772 (2)	173 (3)
O(*W*)—H*a*···O1	1.83 (1)	2.706 (2)	176 (3)
O(*W*)—H*b*···O3^{vii}	1.95 (2)	2.793 (2)	159 (3)
O1′—H1′···O11′	1.69 (2)	2.530 (2)	156 (3)
O3′—H3′···O(*W′*)^{vi}	2.00 (2)	2.868 (2)	177 (3)
O11′—H11′···O(*W*)^{iv}	1.91 (2)	2.748 (2)	163 (3)
O(*W′*)—H*a′*···O1′	1.86 (2)	2.709 (2)	165 (3)
O(*W′*)—H*b′*···O3′^{v}	2.02 (2)	2.887 (2)	171 (3)

† Equivalent positions: (i) $x, y+1, z$; (ii) $2-x, y+\frac{1}{2}, 1-z$; (iii) $2-x, y-\frac{1}{2}, 1-z$; (iv) $1-x, y-\frac{1}{2}, 1-z$; (v) $x, y-1, z$; (vi) $-x, y+\frac{1}{2}, 1-z$; (vii) $1-x, y+\frac{1}{2}, 1-z$.

with two hydroxyl substituents, is directed towards the screw axis, while the hydrophobic edges of the layers formed by $=CH_2$ groups protrude from the terminal pyrane rings. Within a layer, each ring A is linked *via* its O1—H1 and O3—H3 hydroxyl groups to two symmetry-related water molecules, which close a 12-membered ring (hereinafter TMR) with the O3^{a}—H3^{a} group of a second steroid molecule. Every water molecule is coordinated tetrahedrally by four O atoms: three belong to the same TMR, while the fourth is located in an adjacent (symmetry-independent) layer. Finally, in each TMR there are four H atoms which form four hydrogen bonds of OH···O type (Table 1, Fig. 1). However, while the graph sets (Etter, 1990; Bernstein *et al.*, 1995) for the TMRs (denoted *a*1, *a*2, *b*1 and *b*2) are the same, $R_4^4(12)$, the donor and acceptor functions of the bridgehead atoms are somewhat different (Fig. 2). In TMRs *a*2 and *b*1 the sequences of donor/acceptor functions are identical, but differ from those assumed in *a*1 and *b*2. In the latter two rings, the sequences are the same but reversed. In *b*2 the torsion angle C2—C3—O3—H3 is synperiplanar, whereas in each of the three other TMRs it is antiperiplanar. Although they display relatively similar layouts (Fig. 1), the folding of the four molecular layers is different. As shown by the dihedral angle (δ) formed by the best planes of atoms O3—C3—C2—C1—O1 (pertaining to ring A) and O(*W*) with that of O3, O3^{a}, O(*W*) and O(*W*^{b}), layers *A*1 [δ = 57.7 (1)°] and *A*2 [δ = 51.6 (1)°] are folded around the screw axes, *B*1 [δ = 14.9 (2)°] is flattened, while *B*2 assumes a transitional state with δ = 35.1 (4)°. These layer folding differences cannot be correlated with conformational differences

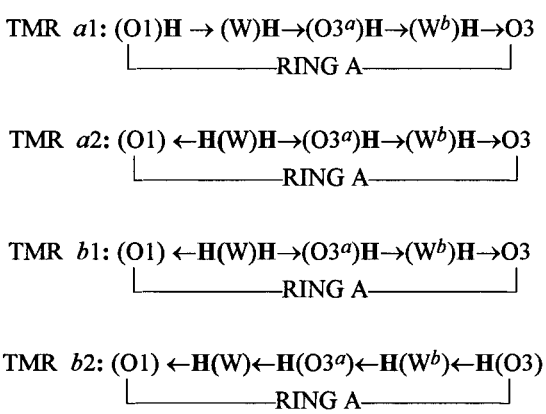

Fig. 2. Distribution of donor–acceptor functions in the four 12-membered rings (TMR).

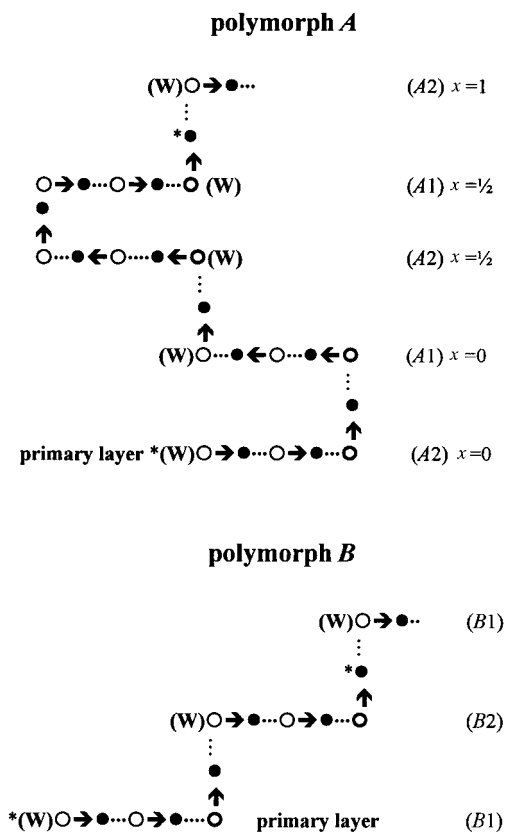

Fig. 3. Connectivity diagrams (***A*** and ***B***) of hydrogen bonds through the independent layers. In dimorph ***A***, four layers are linked by two subsequent homomolecular (hydroxyl → hydroxyl and water → water) pairs, while in ***B*** there are only two heteromolecular hydroxyl → water bonds.

exhibited by the flexible Δ^5 ring B; that is, it assumes an envelope shape in *A*1 and *B*1, whereas it is a half-chair in *A*2 and *B*2.

In spite of such folding differences, the two polymorphs have similar (primary) layers (*A*2 and *B*1) with the same hydrogen bonding, while the accompanying second layers (*A*1 and *B*2) differ in hydrogen bonding from each other and from the primary layers. These layers self-organize by pairs in two types of close packing. In form ***A***, layers (*A*1/*A*2) are stacked upon each other approximately perpendicular to the *a* axis, whereas in form ***B***, layer *B*1 is glide-related to *B*2 by *ca* 1/6 of the $a+c$ diagonal.

2.2. *Layer connectivity*

In dimorph ***B***, the fourth ligand of both water tetrahedra is an O11—H11 hydroxyl group from an adjacent layer (*B*1 or *B*2 and *vice versa*), which donates a short hydrogen bond to the respective water oxygen (Table 1). Simultaneously, these interlayer O11—H11 donors are the recipients of intramolecular hydrogen bonds from the vicinal O1—H1 groups. The latter are then the acceptors of hydrogen bonds from water molecules within their own TMRs. This array is depicted in Fig. 3 as follows. A $C_6^6(12)$ chain formed by two times three consecutive hydrogen bonds starts from a water molecule embedded in a primary layer *B*1 and, passing through layer *B*2, ends up at the water molecule of a second primary layer. This periodical motif ($\Delta x = 1$), in accordance with the position of the screw axes, seems to account for the flattened *B*1 and the slightly folded *B*2 sheets, stacked parallel to the 101 plane (Fig. 4).

In contrast, in dimorph ***A***, the folded *A*1 and *A*2 sheets are stacked parallel to the 100 plane (Fig. 5). This stacking is also cross-bound by a hydrogen-bond chain. It starts from the primary layer *A*2 to the juxtaposed *A*1 layer, but now the acceptor is O11 (Fig. 3). Consequently, within the next three hydrogen bonds formed in layer *A*1 ($x = 0$) the donor/acceptor functions are inverted. This rearrangement unavoidably ousts one of the water hydrogens from layer *A*1, which is then directed toward the next layer *A*2 at $x = \frac{1}{2}$. A full period of the chain (running from asterisk to asterisk in Fig. 3) is completed only after a second two times three hydrogen bonds with *A*2 at $x = 1$, which can be described by a 'double graph' $C_{12}^{12}(24)$ with respect to $C_6^6(12)$ found in form ***B***.

It is noteworthy that the orientation of water molecules in layer *A*1 may also arise from a lack of neighbouring O1—H1 groups. Hypothetically, such a possibility may be realised by the presence of 3β,11α-dihydroxyspirosta-5,25(27)-diene (Ribár *et al.*, 1986) as a minor impurity of 1β,3β,11α-trihydroxyspirosta-5,25(27)-diene [separable from each other by layer chromatography (Vladimirov *et al.*, 1991)]. At present, this hypothesis cannot be disproved; therefore it is to be checked by cocrystallizations.

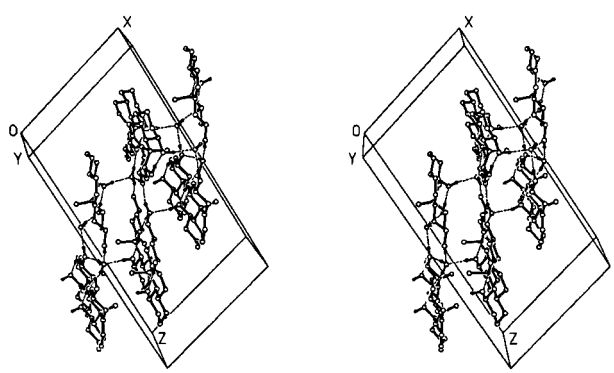

Fig. 4. Stereoview of the crystal packing in dimorph ***B***. For clarity, the steroid molecules are truncated to rings *A*, *B* and *C*.

2.3. *Study of non-bonded interactions*

In addition to the comparison of hydrogen bonds developed in dimorphs ***A*** and ***B***, a visual representation of all of the interatomic interactions was prepared by a new method: *NIPMAT* (Rowland, 1995). As suggested by Desiraju (1996), a pictorial matrix is formed using the atoms of the molecular skeleton of $C_{27}H_{40}O_5$ plus water units ($A_1, A_2, \ldots, A_m, \ldots, A_n$) and the matrix element $A_m - A_n$, which is defined by the shortest intermolecular contacts $A_m \cdots A_n$, is shown as a gray scale. The shorter the contact, the grayer the square which represents that particular contact. However, in contrast to 1,4-benzoquinone and fluoranil, presented by Desiraju (1996), for which both symmetric matrices are of $12^2 = 144$ elements, in our case the two matrices each have $150^2 = 22\,500$ elements, which could not be handled as a whole. Thus both structures were partitioned in terms of the binary layers described. Since the number of elements of each submatrix is still $75^2 = 5625$, the maps, like a scattergram, are rather diffuse.† Remarkably, the gray contacts around the sums of the van der Waals radii of C, O and H are more sporadic and paler within the symmetric submatrices for layers *A*1 and *A*2 than in those calculated for *B*1 and *B*2, respectively. The cross-connections between molecules from layers *A*1–*A*2 and *B*1–*B*2 gave two asymmetric matrices in which the numbers of pale but gray C···H contacts were practically the same (about 110), but in the *B*1–*B*2 matrix the darkest spots slightly outnumber those counted in matrix *A*1–*A*2. With different distribution, the number (about 80) and darkness of the H···H contacts cannot permit substantial differentiation. These observations altogether seem to support the conclusion concerning the greater stability of dimorph ***B***.

† These maps (six in total) and the corresponding atomic numbering scheme of the symmetry-independent molecules can be obtained from LF on request (e-mail: lfabian@cric.chemres.hu).

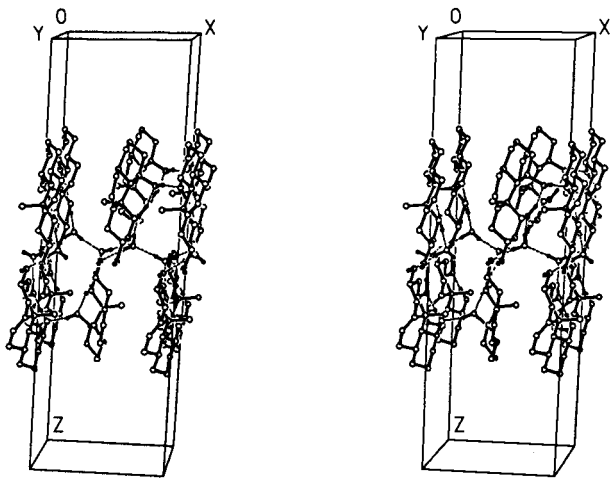

Fig. 5. Stereoview of the crystal packing in dimorph ***A***. For clarity, the steroid molecules are truncated to rings *A*, *B* and *C*.

3. Conclusions

The dimorphs ***A*** and ***B*** have one type of steroid–water layer in common (Fig. 1): such layers have identical sequences of hydrogen-bond donor/acceptor functions (TMRs *a*2 and *b*1). These layers differ only in their folding, which is more pronounced for layer *A*2 than for *B*1. Then with different water rotations, each forms its own complementary sheet, *A*1 or *B*2, respectively. In dimorph ***B***, water molecules are rotated around the O(*W*)—H*a*···O1 bonds by *ca* 180°. These turns direct the other protons (H*b*) towards O3—H3 radicals in unison with rotations about the C3—O3 bonds (torsion angle C2—C3—O3—H3 moves from anti- to syn-periplanar). This reverses the hydrogen-bond helix in layer *B*2 around the screw axis compared to the other three layers.

In layer *A*1, the water molecule rotates around the O(*W*)—H*b*···O3 hydrogen bond, but only by ∼90°. This turn enables the second hydrogen (H*a*) to establish a connection to the water molecule embedded in layer *A*2. This rearrangement inverts simultaneously the hydrogen bonds between O(*W*), O1 and O11, resulting in a basically different packing (Fig. 5) from that observed in dimorph ***B*** (Fig. 4). In dimorph ***A***, four subsequent layers stacked upon each other along the *a* axis are cross-linked by two homomolecular (hydroxyl···hydroxyl and water···water) hydrogen-bond pairs, while in the higher melting-point form there are only heteromolecular hydroxyl···water bonds between the *B*1→*B*2→*B*1 layers; the latter are mutually glide-related along the 101 plane.

The authors thank one of the referees for his suggestion to apply the program *NIPMAT*, which was kindly provided by Dr R. S. Rowland (Birmingham, Alabama). Thanks are also due to Professor B. Ribár (Novi Sad) and Dr S. M. Vladimirov (Belgrade) for additional information on the crystals. This work has been sponsored by the Hungarian Research Fund Grant No. OTKA T023212.

References

Argay, Gy., Kálmán, A., Zivanov-Stakic, D., Vladimirov, S. & Ribár, B. (1998). *Acta Chim. Hung.* **135**, 449–456.
Bernstein, J., Davis, R. E., Shimoni, L. & Chang, N.-L. (1995). *Angew. Chem. Int. Ed. Engl.* **34**, 1555–1573.
Bernstein, J. & Henck, J.-O. (1998). *Cryst. Eng.* **1**, 119–128.
Czugler, M., Kálmán, A., Kovács, J. & Pintér, I. (1981). *Acta Cryst.* B**37**, 172–177, and references therein.
Desiraju, G. R. (1996). *Acc. Chem. Res.* **29**, 441–449.
Dunitz, J. D. & Bernstein, J. (1995). *Acc. Chem. Res.* **28**, 193–200.
Etter, M. C. (1990). *Acc. Chem. Res.* **23**, 120–126.
Griesser, U. J., Burger, A. & Mereiter, K. (1997). *J. Pharm. Sci.* **86**, 352–358.
Haleblian, J. K. (1975). *J. Pharm. Sci.* **64**, 1269–1287.
Hegedüs, B., Bod, P., Harsányi, K., Péter, I., Kálmán, A. & Párkányi, L. (1989). *J. Pharm. Biomed. Anal.* **7**, 563–569.
Kálmán, A., Argay, Gy., Ribár, B., Zivanov-Stakic, D. & Vladimirov, S. (1985). *Acta Cryst.* C**41**, 1645–1647.
Ribár, B. (1984). Personal communication.
Ribár, B., Kapor, A., Vladimirov, S., Zivanov-Stakic, D., Argay, Gy. & Kálmán, A. (1986). *Acta Cryst.* C**42**, 1780–1782.
Rowland, R. S. (1995). *Am. Crystallogr. Assoc. Abstr.* **23**, 63.
Threlfall, T. L. (1995). *Analyst*, **120**, 2435–2460.
Vladimirov, S. (1998). Personal communication.
Vladimirov, S., Zivanov-Stakic, D. & Ribár, B. (1991). *Phytochemistry*, **30**, 1724–1725.